SUPPORTING INFORMATION

Self-folding graphene scaffolds with integrated electronics for cardiac tissue engineering

Alonso Ingar Romero,[1,2,3,7] Koji Sakai, [3,4] Toichiro Goto,[3,4] George Al Boustani,[1,2,7] Ryuya Kida, [1,2,7] Defne Tüzün, [1,2,7] Yuta Tanimura,[2] Ann-Caroline Heiler,[5,6,7] Joe Alexander, [1] Andreas R. Bausch,[5,6,7] Bernhard Wolfrum,[1,2,7] Tetsuhiko F. Teshima[*1,2,7,8]*

AUTHOR AFFILIATIONS

1 Medical & Health Informatics Laboratories, NTT Research Incorporated, Sunnyvale, CA, 94085 USA

2 Neuroelectronics, Munich Institute of Biomedical Engineering, Department of Electrical Engineering, TUM School of Computation, Information and Technology, Technical University of Munich, Garching, Germany

3 Basic Research Laboratories, NTT, Inc., 3-1 Morinosato Wakamiya, Atsugi, Kanagawa 243-0198, Japan

4 NTT Bio-Medical Informatics Research Center, NTT, Inc., 3-1 Morinosato Wakamiya, Atsugi, Kanagawa 243-0198, Japan

5 Heinz Nixdorf Chair in Biophysical Engineering of Living Matter, Garching, Germany

6 Center for Functional Protein Assemblies (CPA), Technical University of Munich, Garching, Germany

7 Center for Organoid Systems (COS), Technical University of Munich, Garching, Germany

8 Department of Mechanical Engineering, Faculty of Science and Technology, Keio University, 3-14-1 Hiyoshi, Kohoku-ku, Yokohama, 223-8522, Japan

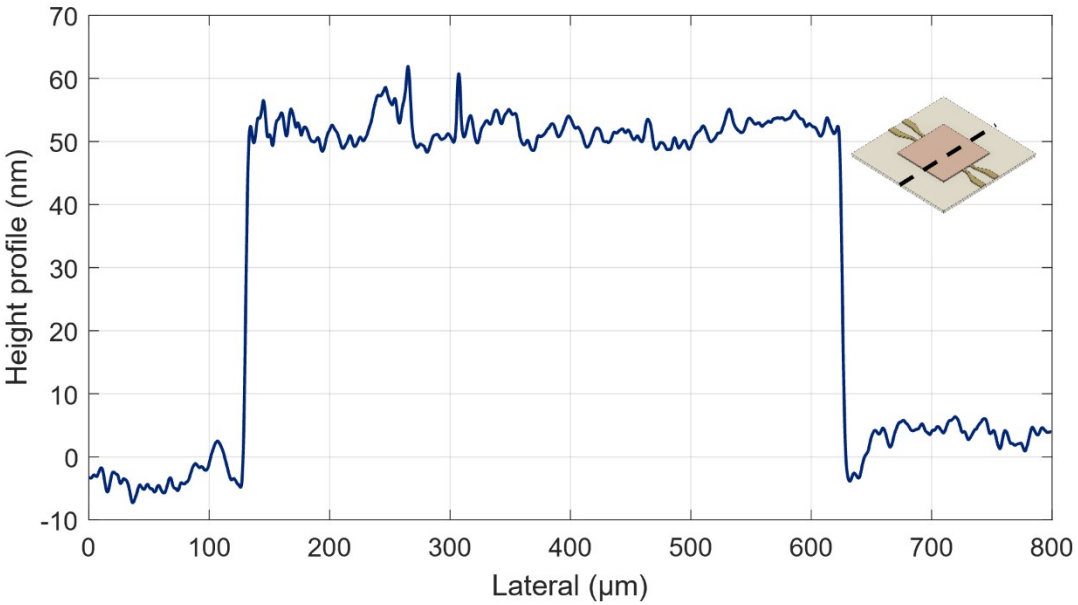

Figure S1. Profilometer measurement of the patterned Ca-alginate layer along the dashed line of the top-right schematic.

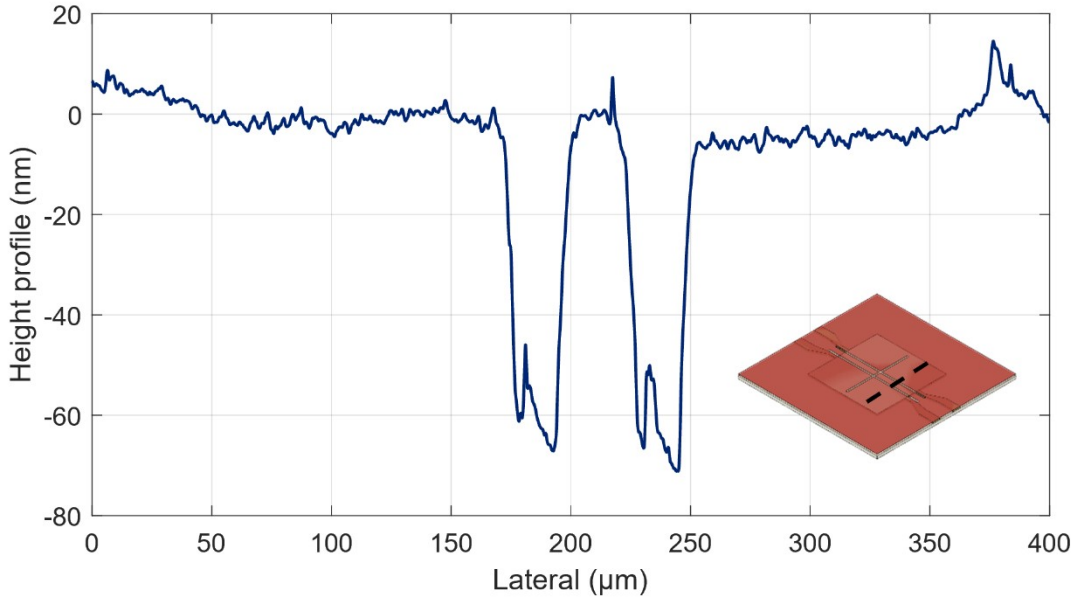

Figure S2. Profilometer measurement of the patterned graphene layer on top of Ca-alginate along the dashed line at the bottom-right schematic.

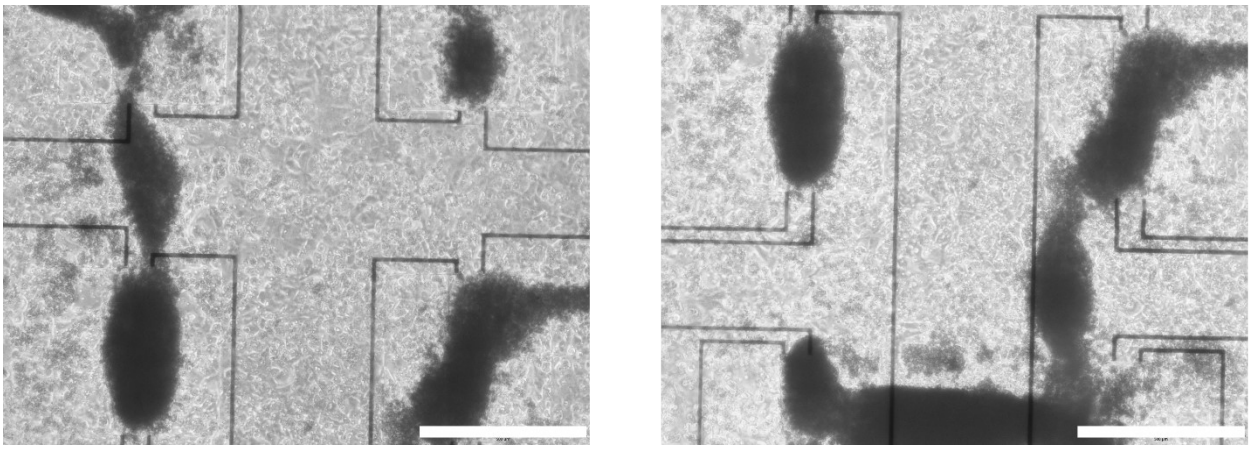

Figure S3. Cellular connections between different aggregates of primary cardiomyocytes around the graphene micro-rolls. Scale bar: 500 μm.

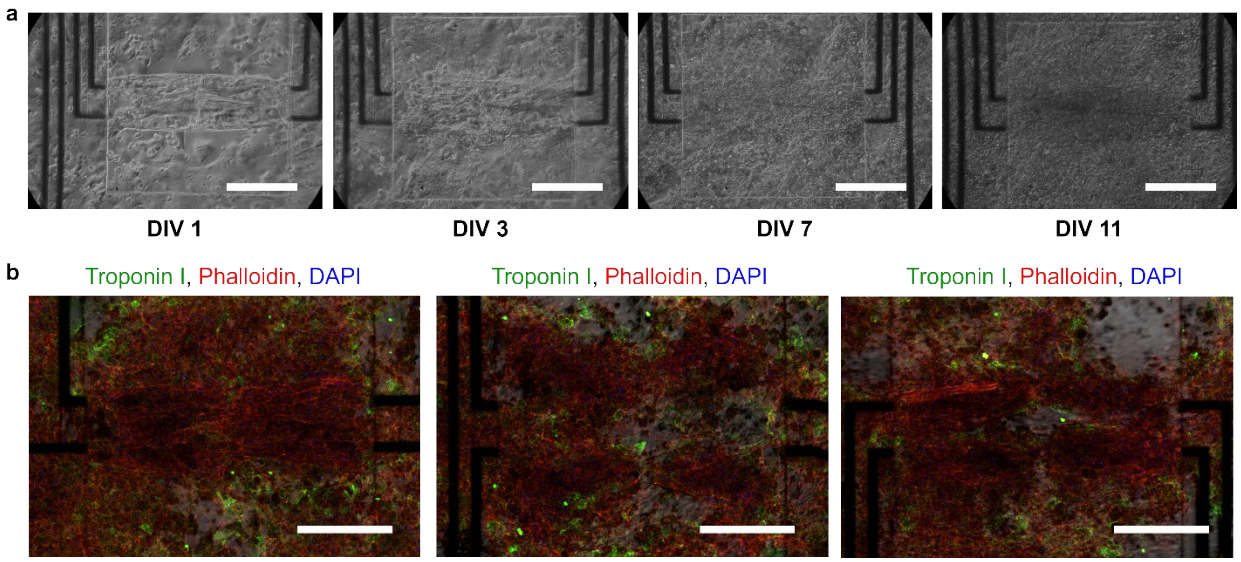

Figure S4. Long-term morphological and immunofluorescent characterisation of HL-1 cardiomyocytes cultured on graphene micro-roll scaffolds. (a) Time-lapse phase-contrast images showing the evolution of HL-1 cardiomyocyte cultures on graphene micro-rolls during the first 11 days. The images demonstrate stable cell attachment and progressive tissue coverage of the scaffold. (b) Immunofluorescence staining of HL-1 cardiomyocytes cultured on micro-rolls showing troponin I (green), phalloidin (actin cytoskeleton, red), and DAPI (nuclei, blue), confirming the presence of organised contractile structures within the cell network. Images were acquired from three representative micro-roll scaffolds at DIV 10. Scale bar: 200 μm.

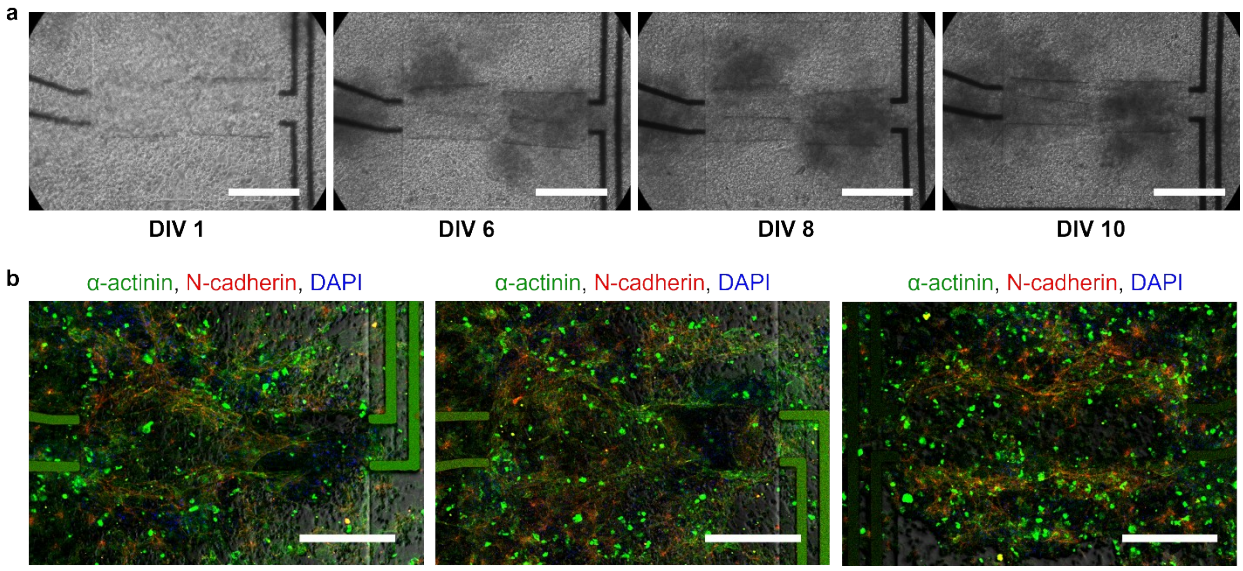

Figure S5. Long-term culture and structural characterisation of hiPSC-CMs on graphene micro-roll scaffolds. (a) Time-lapse phase-contrast images of hiPSC-CMs cultured on graphene micro-rolls during the first 10 days, demonstrating stable attachment and network formation on the scaffold surface.
(b) Immunofluorescence staining of hiPSC-CMs showing α-actinin (sarcomeric marker, green), N-cadherin (cell–cell junctions, red), and DAPI (nuclei, blue), illustrating the formation of cardiomyocyte networks and intercellular junctions on the micro-roll scaffold at DIV 8. Images are representative of three independent micro-roll devices. Scale bar: 200 μm.

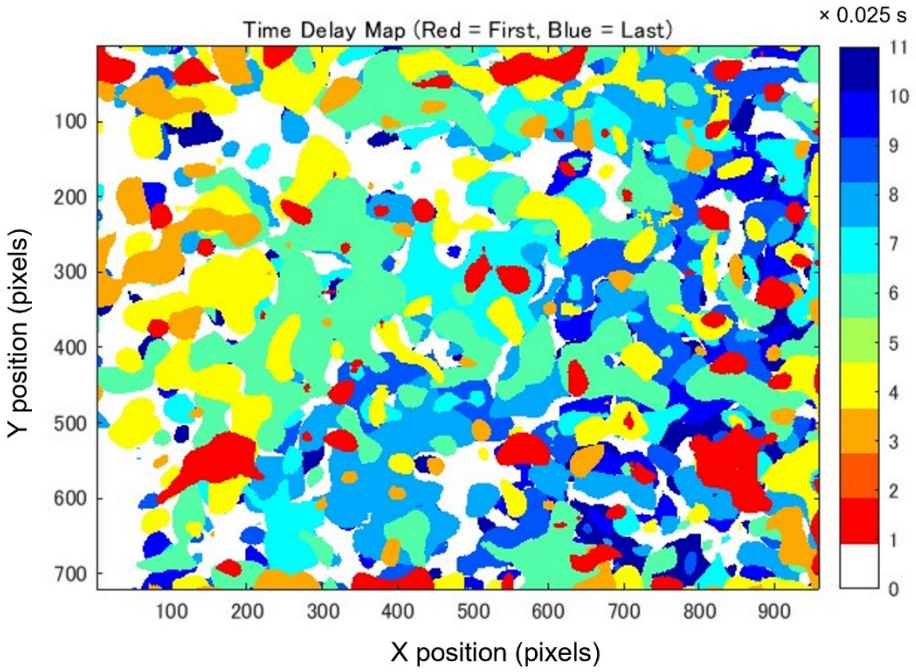

Figure S6. Spatial map of activation delays derived from Ca^{2+} imaging recordings of HL-1 cells at DIV 11 (Movie S4). Each pixel represents the relative activation time of the Ca^{2+} transient, with colour indicating the temporal delay (red = earliest activation, blue = latest activation). The colour scale is expressed in increments of 0.025 s. While the map reveals spatial heterogeneity in activation timing across the recorded field, a clear trend can be identified which propagates from top left to bottom right. Based on this observation, we estimate a propagation velocity of around 7 mm s^{-1}.

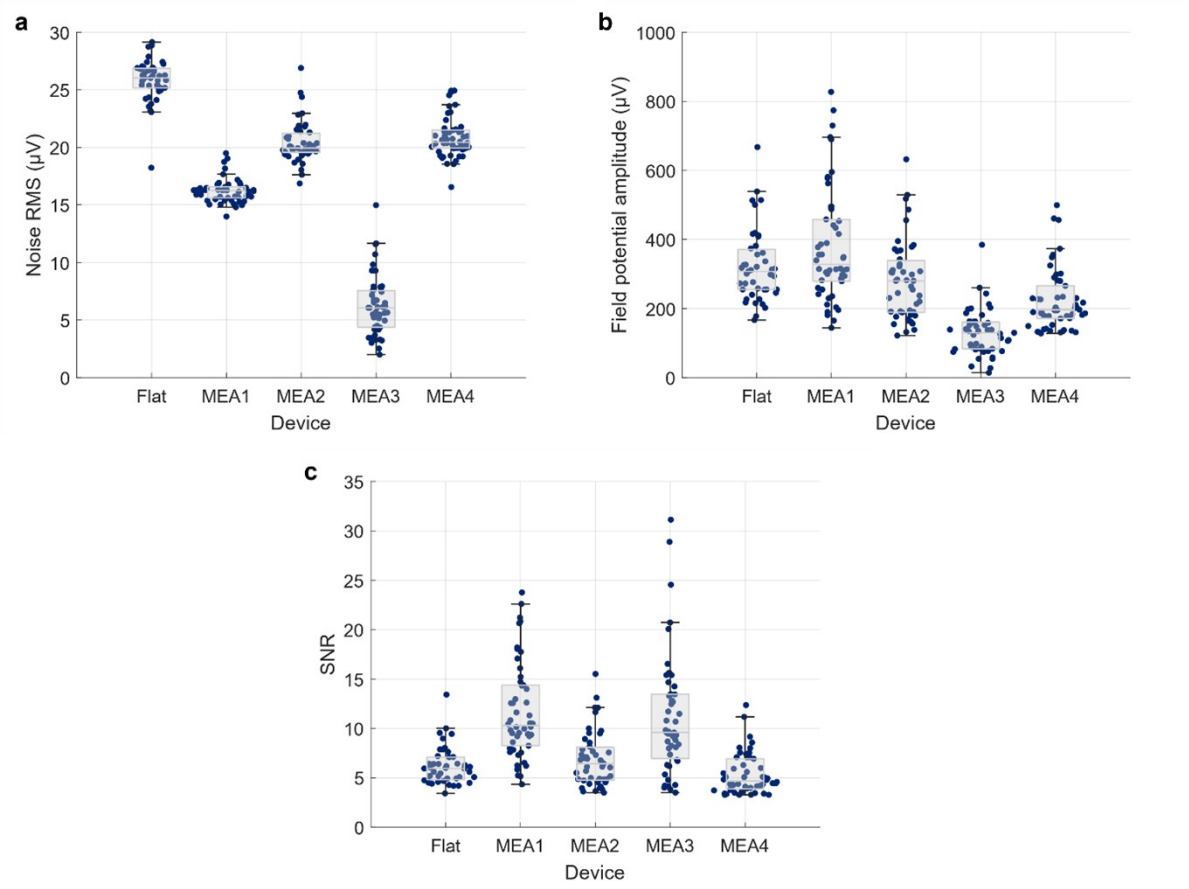

Figure S7. Within-array variability of electro-performance metrics. (a) Noise RMS ($^{V_{RMS}}$), (b) Peak-to-peak field potential amplitude ($^{V_{pp}}$) and (c) SNR distributions calculated from all channels across 4 graphene micro-roll MEAs at DIV 6 (n = 183 channels) as well as side-by-side comparison with a planar graphene MEA (n = 42 channels).

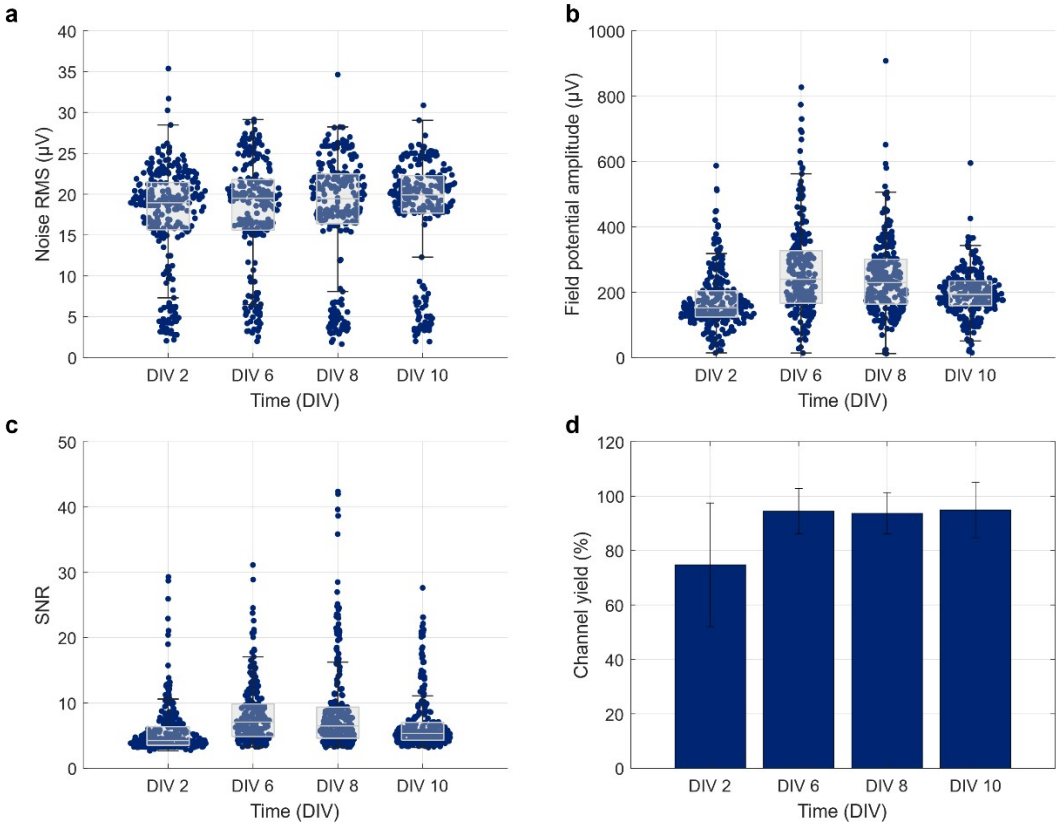

Figure S8. Stability over time of electro-performance metrics. (a) Noise RMS, (b) Peak-to-peak field potential amplitude, (c) SNR distributions and (d) biologically active channel yield calculated from all channels across 4 graphene micro-roll MEAs for 8 days. A channel was considered active if it featured an SNR ≥ 3.5.

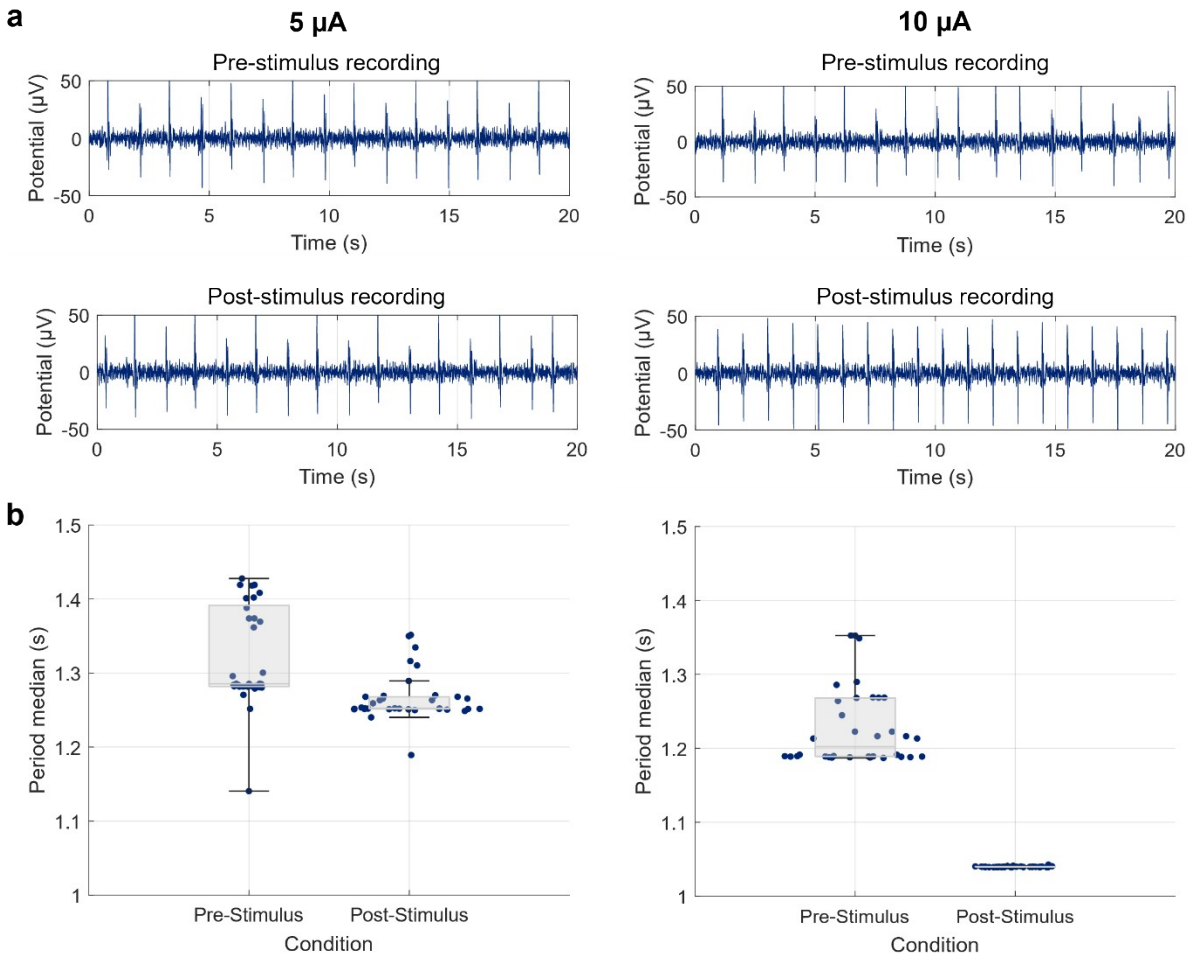

Figure S9. Amplitude dependent response of HL-1 cells induced by 1 Hz electrical stimulation. (a) Representative recordings from a single channel 20 s before and 20 s after 10 biphasic stimuli. Stimulation at 10 µA resulted in a transient synchronization of the beating frequency to approximately 1 Hz following the stimulation train, whereas stimulation at 5 µA did not induce a notable change in beating rate. (b) Swarm plot of the median beating period of all active electrodes of the device before and after stimulation, indicating a stimulation-amplitude-dependent modulation of network activity.

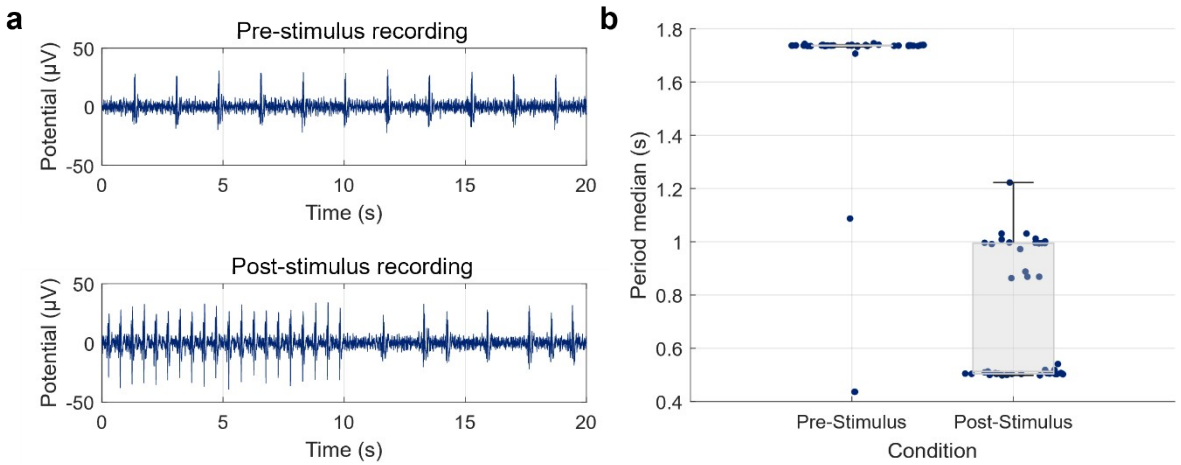

Figure S10. Entrainment-like response to 2 Hz electrical stimulation. (a) Representative recording 20 s before and 20 s after application of a train of 10 biphasic current pulses (2 Hz, 60 µA). While stimulus-evoked responses during the pulse are obscured by the stimulation artifact, many electrodes exhibited a transient increase in beating frequency to approximately 2 Hz following the stimulation train. (b) Swarm plot of the median beating period across all active electrodes of the device before and after stimulation. While the majority of channels followed the 2 Hz stimulation frequency, some electrodes synchronised at approximately 1 Hz, indicating partial entrainment of the network activity.

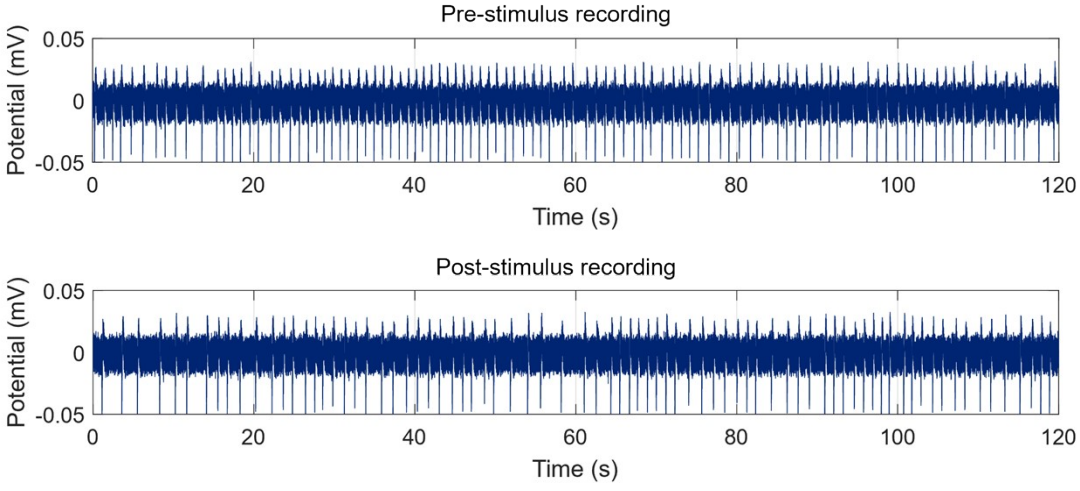

Figure S11. Raw spontaneous electrical activity of primary cardiomyocytes before and after applying a 2-s periodic stimulus corresponding to the average period analysis shown in Figure 5a.

ATTACHED CONTENT

Supplementary movie 1. Primary cardiomyocyte culture beating around graphene scaffolds at DIV 2. (MP4)

Supplementary movie 2. 3D z-stack animation of the immunostained low cell density graphene micro-roll in Figure 3b (middle). (MP4)

Supplementary movie 3. 3D z-stack animation of the immunostained high cell density graphene micro-roll in Figure 3b (right). (MP4)

Supplementary movie 4. Exemplary Ca^{2+} imaging recording of HL-1 cells at DIV 11. (MP4)